Original Article

Effect of microenvironment on adhesion and differentiation of murine C3H10T1/2 cells cultured on multilayers containing collagen I and glycosaminoglycans

Journal of Tissue Engineering
Volume 11: 1–16

DOI: 10.1177/2041731420940560
journals.sagepub.com/home/tej
SAGE

Mingyan Zhao[1], Reema Anouz[2] and Thomas Groth[2,3,4]

Abstract

Polyelectrolyte multilayer coating is a promising tool to control cellular behavior. Murine C3H10T1/2 embryonic fibroblasts share many features with mesenchymal stem cells, which are good candidates for use in regenerative medicine. However, the interactions of C3H10T1/2 cells with polyelectrolyte multilayers have not been studied yet. Hence, the effect of molecular composition of biomimetic multilayers, by pairing collagen I (Col I) with either hyaluronic acid or chondroitin sulfate, based primarily on ion pairing and on additional intrinsic cross-linking was studied regarding the adhesion and differentiation of C3H10T1/2 cells. It was found that the adhesion and osteogenic differentiation of C3H10T1/2 cells were more pronounced on chondroitin sulfate-based multilayers when cultured in the absence of osteogenic supplements, which corresponded to the significant larger amounts of Col I fibrils in these multilayers. By contrast, the staining of cartilage-specific matrixes was more intensive when cells were cultured on hyaluronic acid-based multilayers. Moreover, it is of note that a limited osteogenic and chondrogenic differentiation were detected when cells were cultured in osteogenic or chondrogenic medium. Specifically, cells were largely differentiated into an adipogenic lineage when cultured in osteogenic medium or 100 ng mL^{-1} bone morphogenic protein 2, and it was more evident on the oxidized glycosaminoglycans-based multilayers, which corresponded also to the higher stiffness of cross-linked multilayers. Overall, polyelectrolyte multilayer composition and stiffness can be used to direct cell–matrix interactions, and hence the fate of C3H10T1/2 cells. However, these cells have a higher adipogenic potential than osteogenic or chondrogenic potential.

Keywords

Biomimetic multilayers, glycosaminoglycans, collagen I, intrinsic cross-linking, C3H10T1/2 cells, cell adhesion and differentiation

Date received: 15 May 2020; accepted: 18 June 2020

Introduction

In vivo, cells reside in an extracellular matrix (ECM)-based microenvironment consisting of fibril-forming proteins, such as collagens, laminin, and fibronectin,[1] making the insoluble protein component of the ECM and polysaccharide-based on glycosaminoglycans (GAGs) in particular hyaluronan and proteoglycans, which contain other GAGs such as chondroitin sulfate (CS), heparan sulfate, and others.[2] In addition, various cytokines as soluble protein components are contained in the ECM or bound to the cell surface by support from sulfated GAGs.[3] The ECM proteins can interact with cells via integrin

[1]Stem Cell Research and Cellular Therapy Center, Affiliated Hospital of Guangdong Medical University, Zhanjiang, China
[2]Department Biomedical Materials, Institute of Pharmacy, Martin Luther University Halle Wittenberg, Halle (Saale), Germany
[3]Laboratory of Biomedical Nanotechnologies, Institute of Bionic Technologies and Engineering, I.M. Sechenov First Moscow State University, Moscow, Russian Federation
[4]Interdisciplinary Center of Materials Research, Martin Luther University Halle Wittenberg, Halle (Saale), Germany

Corresponding author:
Mingyan Zhao, Stem Cell Research and Cellular Therapy Center, Affiliated Hospital of Guangdong Medical University, Zhanjiang 524001, China.
Email: mingyan.zhao@gdmu.edu.cn

adhesion receptors,[4] which are involved in cell signaling transduction, and thus influencing cell adhesion, growth, and differentiation.[5] Moreover, interaction of proteoglycans having GAGs side-chains of heparin and CS, but also fibronectin with growth factors (GFs) including bone morphogenic proteins (BMPs) provides the basis for GF-related signal transduction processes, too.[2,6] Hence, the ECM acts not only as a structural support of cells, but provides chemical and mechanical cues involved in the regulation of cellular responses.[6,7]

Biomaterials for use as scaffolds in tissue engineering should meet important characteristics, such as bioactivity and biodegradability. Many synthetic materials such as polylactic or polyglycolic acids have been widely used because of their good mechanical properties, low cost, and biodegradability.[8] However, those synthetic materials have poor bioactive properties, because they lack the necessary cues to guide cellular behavior in a desired manner.[9] Furthermore, the bio-integration, which is the interaction between an implant and the host tissue, occurs always at the interface or surface of the implant materials.[10] Therefore, despite the importance of bulk properties of a biomaterial, the surface properties arise to play a critical role in the process.[11] Hence, several physiochemical surface modification methods have been established to alter the surface properties of biomaterials in a desired manner. While physical and chemical treatments of implant materials often modulate biocompatibility to improve engrafting or reduce adverse effects, biomimetic modifications aim at reestablishing an ECM-like microenvironment for tissue cells[12] to resemble the mechanical and chemical cues required to control cell behavior and tissue regeneration.[13]

Among a variety of methods for surface modification, layer-by-layer (LbL) assembly of polyelectrolytes has emerged as a very simple, cost-efficient, and versatile strategy in fabricating biogenic thin films and for the immobilization of bioactive molecules such as growth factors on biomaterial surfaces.[14–16] Matrix components such as fibrillar glycoproteins (e.g. collagens, fibronectins, laminins) and GAGs such as CS, heparin, and HA have gained an increasing interest for making of bioactive surface coatings and three-dimensional (3D) systems,[15,17,18] implementing that as a step toward mimicking the native ECM. However, some of these polysaccharide and protein-based multilayer systems have been found to be relatively unstable under physiological conditions[19] that may require subsequent or concurrent cross-linking to improve their stability. To enhance stability of multilayers from biogenic polyelectrolytes, we introduced recently intrinsic cross-linking by formation of imine bonds between aldehydes of oxidized GAGs with pendant amino groups of proteins resulting in improved stability.[20]

Mesenchymal stem cells (MSCs) represent a multipotent type of cells, which lineages result in all kinds of connective tissues. Hence, they have been considered for regenerative therapies of musculoskeletal diseases and traumata.[21] Indeed, programming of MSCs differentiation has been done by tailoring physical and chemical cues expressed by man-made material surfaces including application of ECM components[22] and growth factors.[23] However, proliferative capacity of MSCs is limited to a few passages[24] and studies of fundamental effects of surface modifications may be hampered by use of several passages and donors. However, cell lines derived from multipotent mesenchymal cells such as the C3H10T1/2 cell line established in 1973 from C3H mouse embryos of 14- to 17-day-old mice[25] that share many features of MSCs, may be an alternative source of cells for studies on development of biomimetic surfaces for tissue engineering of bone, cartilage, and other types of connective tissues. In fact, C3H10T1/2 cells are able to develop into different cell lineages under specific cell culture induction media including osteoblasts,[26] chondrocytes,[27] and also adipocytes.[28] For example, bone morphogenic protein 4 (BMP-4) has been found to promote the adipogenic differentiation of C3H10T1/2 cells[28] while a high cell density micro-mass culture with a specific medium (supplemental with a purified mixture of osteoinductive proteins, ascorbic acid, and β-glycerophosphate) regulates commitment to the chondrogenic lineage.[27] In addition, previous studies found that BMP-2 was capable of triggering commitment of multipotent C3H10T1/2 cells to adipocyte[29] and osteocyte[26] lineages. Moreover, others observed that these cells respond to chemical and mechanical cues differentiating into osteoblasts, chondrocytes, and tenoblasts.[30] Hence, they seem to represent a suitable model to study the effect of biomimetic surface modifications on differentiation of multipotent cells.

So far, the effect of composition of biomimetic multilayers that resemble matrix composition of connective tissues such as bone and cartilage using collagen and either CS or HA on differentiation of C3H10T1/2 cells has not been studied yet. In addition, no studies exist that investigate the effect of intrinsic cross-linking of multilayers on adhesion, growth, and differentiation of C3H10T1/2 cells. Hence, in the present work, biomimetic multilayers prepared by pairing collagen I (Col I) with HA or CS in either native or oxidized form were used as substrate for studying adhesion, growth, and multipotent differentiation of C3H10T1/2 cells to learn about the effect of ECM-like microenvironment of differentiation of multipotent cells into mesenchymal tissues.

Materials and methods

Materials

Glass coverslips (Roth, Germany) of size Ø12 mm and Ø15 mm were treated with 0.5 M sodium hydroxide (Roth) dissolved in 96% ethanol (Roth) to clean the surfaces for

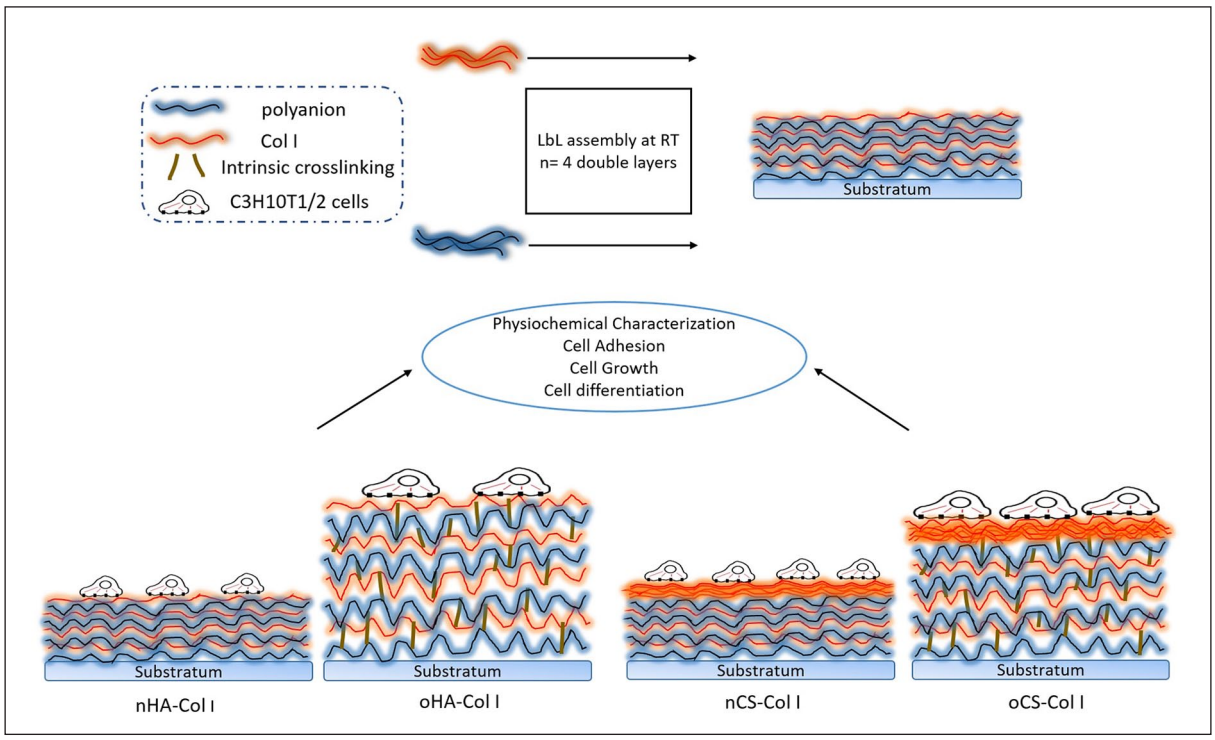

Figure 1. A concept figure illustrating the differences among the four multilayer systems.

2 h at room temperature. Subsequently, the samples were thoroughly washed with ultrapure water and dried under nitrogen flow. Silicon wafers (Silicon materials, Germany) were cut to a size of (10×10) mm^2 and (37×17) mm^2 and cleaned with a solution of hydrogen peroxide (35%, Roth), ammonium hydroxide (25%, Roth), and ultrapure water (1:1:5, v/v/v) at 75°C for 15 min.[31] Thereafter, the wafers were thoroughly rinsed with ultrapure water and dried with nitrogen. New gold-coated quartz sensors (QT Quarztechnik GmbH, Germany) for quartz crystal microbalance (QCM) measurements were cleaned with ethanol p.a. (99.8%, Roth), and extensively rinsed with ultrapure water. After drying with nitrogen, the sensors were kept in 2 mM mercaptoundecanoic acid (MUDA, 95%, Sigma, Germany) diluted in ethanol p.a. at room temperature to obtain a negatively charged surface overnight owing to the formation of carboxylate-terminated monolayer.[32]

Native hyaluronic acid (nHA MW ~ 1.3 MDa) was provided by Innovent (Jena, Germany) while native chondroitin sulfate (nCS, MW ~ 25 kDa) was purchased from Sigma. Polyelectrolyte solutions were prepared as follows: poly (ethylene imine) (PEI, MW ~ 750 kDa, Sigma, Germany) was dissolved in a 0.15 M sodium chloride (NaCl, Roth) solution at a concentration of 5 mg mL^{-1} and adjusted to a pH value of 7.4. The native and oxidized GAGs (nGAGs and oGAGs) were used as polyanions and were dissolved under stirring in a 0.15 M sodium chloride to obtain a final concentration of 0.5 mg mL^{-1}. Collagen I (Col I) from porcine skin (polycation, MW ~ 100 kDa, Sichuan Mingrang Bio-Tech, China) was used as polycation and was dissolved in 0.2 M acetic acid (Roth) at a concentration of 2 mg mL^{-1} at 4°C. After dissolution, the Col I solution was centrifuged at 9000*g* for 10 min and then diluted to a final concentration of 0.5 mg mL^{-1} using 0.2 M acetic acid supplied with NaCl (final concentration to 0.15 M NaCl). The pH value of the polyelectrolyte solutions was adjusted to pH 4.0.

Polyelectrolyte multilayer assembly

Cleaned glass coverslips or silicon wafers were used as substrate for deposition of polyelectrolyte multilayers. A first anchoring layer of PEI was formed on the substrate to obtain a surface with positive charge, which was then followed by adsorption of nGAGs (nCS, nHA) or oGAGs (oCS, oHA) as the anionic layer and then Col I as the cationic layer. Polyelectrolyte multilayers were fabricated by immersing the glass coverslips in polyanions for 15 min while in polycation for 20 min followed by three times rinsing with a solution of NaCl (0.15 M, pH 4.0) for 5 min. By alternating adsorption of Col I and nGAGs or oGAGs, multilayers with eight total layers (eighth) on top of the PEI layer were fabricated. The four different systems (Col I terminated, see Figure 1) were designated as: nHA–Col I, oHA–Col I, nCS–Col I, and oCS–Col I.

Physicochemical characterization of multilayers

The layer growth was monitored in situ using surface plasmon resonance (SPR, iSPR from IBIS Technologies,

Hengelo, The Netherlands), which is based on the detection of changes in the refractive index (RI) caused by the adsorption of molecules at the gold–liquid interface of the sensor. The resulting change in the SPR angle shift (m°) is proportional to the mass (Γ_{SPR}) of adsorbed molecules on the surface given as[33]

$$122\ \text{m}^\circ \approx 1\ \text{ng mm}^{-1} \quad (1)$$

The measurements were performed in situ in the flow cell of the device using gold sensors treated with MUDA (see above). Shifts in resonance angles from 10 regions of interest (ROI) defined on the sensor surface were recorded using the IBIS SPR software. To obtain a stable baseline, 0.15 M NaCl (pH 4.0) was injected into the flow cells. Then, the polyelectrolyte solution was brought to the sensor surface for 15 min followed by 15 min rinsing with 0.15 M NaCl solution (pH 4.0). Afterwards, polyelectrolyte solutions of nGAGs or oGAGs and Col I were adsorbed up to eight layers with incubation times of 15 min for nGAGs and oGAGs, while 20 min for Col I. Each adsorption step was followed by a rinsing step described above to remove unbound or loosely bound material.

QCM measurements were conducted using a LiquiLab 21 (ifak e.V., Germany) with MUDA-modified gold sensors mounted in the flow cells of the device to monitor the damping shift after each single adsorption step. The damping shift reflects the mechanical properties of multilayers with higher values for softer adsorbed mass.[34,35] The flow regime (3 µL s^{-1}) and time periods for pumping the different polyelectrolyte and washing solutions from reservoirs were programmed with the device.

The presence and organization of Col I in multilayers was characterized after in situ labelling with fluorescein isothiocyanate (FITC, Sigma)[36] using a confocal laser scanning microscope (CLSM 710, Carl Zeiss MicroImaging GmbH, Germany). Briefly, the multilayer-coated glass slides were placed in 24-well plates (Greiner, Germany). Then, 500 µL of 0.6 mg mL^{-1} FITC (Sigma) dissolved in pure dimethyl sulfoxide (DMSO, Sigma) solution was added to each well, followed by incubation at room temperature for 10 h. Then, samples were washed extensively with 0.15 M NaCl to remove any residual FITC. After a final short washing with water, samples were mounted with Mowiol (Merck, Germany) and examined with CLSM.

Cell culture

C3H10T1/2 embryonic fibroblasts (Clone 8) were purchased from ATCC (CCL-226, LGC Standards GmbH Wesel, Germany) and grown in Dulbecco's modified Eagle's medium (DMEM, Biochrom AG, Germany) supplemented with 10% fetal bovine serum (FBS, Biochrom AG) and 1% antibiotic–antimycotic solution (AAS, Promocell, Germany) at 37°C in a humidified 5% CO_2/95% air atmosphere. Prior to reaching confluence, the cells were harvested from the culture flasks by treatment with 0.25% trypsin/0.02% EDTA (Biochrom AG) followed by subsequent centrifugation and re-suspending in DMEM at a concentration of 20,000 cells mL^{-1}.

Short-term interaction of C3H10T1/2 cells with multilayers

Cell adhesion and spreading. Adhesion of C3H10T1/2 cells was studied on glass coverslips coated with multilayer coatings of polyanion (nHA, oHA, nCS, oCS) and Col I. The serum-free C3H10T1/2 cell suspensions (1×10^4 cells), were prepared as mentioned above, and seeded on samples and incubated for 4 h. After incubation, the cells were stained with crystal violet (Roth; 0.5% (w/v)) in methanol (Roth) at room temperature for 30 min, and then carefully washed with water and dried in air. Images were taken in transmission mode with an Axiovert 100 (Carl Zeiss MicroImaging GmbH, Germany) equipped with a charge-coupled device (CCD) camera (Sony, MC-3254, AVT-Horn, Germany). Cell count, cell area, and aspect ratio were calculated from five images per sample using image processing software "ImageJ 1.41o, NIH."

Focal adhesion complex formation and organization of cellular integrins. The C3H10T1/2 cell suspensions (1×10^4 cells) were prepared and placed on samples and incubated for 24 h. After incubation, the cells attached to the multilayers were fixed with 4% paraformaldehyde solution (Roth) for 10 min followed by rinsing with phosphate-buffered saline (PBS). Thereafter, the cells were permeabilized with 0.1% Triton X-100 in PBS (v/v; Sigma) for another 10 min and washed again with PBS. The samples were further blocked by incubation with 1% (w/v) bovine serum albumin (BSA, Merck) at room temperature for 1 h. To study the formation of focal adhesions (FA) and distribution of integrins, the samples were stained by incubation with a rabbit polyclonal antibody against α2 (1:100, Santa Cruz, USA) and a mouse monoclonal antibody against vinculin (1:100, sigma), or incubated with a mouse monoclonal antibody against CD44 (1:100, Dianova, Germany) at room temperature for 30 min. After rinsing with PBS, the samples were treated with a goat Cy2-conjugated anti-mouse or goat Cy3-conjugated anti-rabbit secondary antibody (1:100, Dianova) for another 30 min. In addition, actin cytoskeleton was labeled by incubating the samples with BODIPY-phalloidin (1:50, Invitrogen, Germany) at room temperature for 30 min. The samples were then rinsed again with PBS and mounted with Mowiol. Subsequently, the samples were examined using CLSM and images were processed with the ZEN2011 software (Carl Zeiss). The vinculin level in cells was quantified using ImageJ as described in our previous work.[17]

Growth of C3H10T1/2 cells

A total 500 µL (2×10^4 cells mL^{-1}) C3H10T1/2 cells suspended in DMEM with 10% FBS were seeded either on multilayers or plain glass coverslips and cultured for 1, 2, and 3 days. Growth of cells was monitored using a phase contrast microscopy equipped with a CCD camera (Leica, Germany). Images were taken at the different days of culture. The quantity of cells was measured the same day with a Qblue fluorescence assay (BioChain, USA), which quantifies the amount of metabolic active cells. On the measuring day, the old medium was carefully removed and the samples were washed with sterile PBS once. Then, 400 µL of phenol red free DMEM supplemented with 40 µL of Qblue assay reagent was added to each well. After 2 h of incubation at 37°C, 100 µL of supernatant of each well was transferred to a black 96-well plate, and fluorescence intensity (excitation wavelength 544 nm, emission wavelength 590 nm) was measured using a plate reader (BMG LABTECH, Fluostar OPTIMA, Germany).

Cell differentiation

Multi-lineages differentiation induction. For differentiation experiments, 1 mL C3H10T1/2 cells were plated on plain or multilayer-coated glass coverslips at a density of 2.5×10^4 cells mL^{-1}. After the cells reached almost confluence, differentiation was induced with 100 ng mL^{-1} BMP-2; or with osteogenic media (OM) consisting of basal medium (BM, 10% FBS and 1% penicillin–streptomycin-containing DMEM) supplemented with 10 nM dexamethasone (Sigma), 20 mM β-glycerophosphate (Alfa Aesar, USA), 50 µM L-ascorbic acid (Sigma), and 50 ng mL^{-1} BMP-2 (Speed Biosystem, USA); or with chondrogenic media (CM) consisting of BM supplemented with 0.1 µM dexamethasone, 50 µg mL^{-1} L-ascorbic acid, 40 µg mL^{-1} L-proline, and 1% ITS (Sigma). The medium was changed every 3 days until end-point assay. Images were taken using a phase contrast microscopy during the different days of induction.

Alkaline phosphatase activity detection. At day 10 of induction with BM or OM, alkaline phosphatase activity (ALP) was measured to evaluate the osteoblastic differentiation of C3H10T1/2 cells. Cell lysates were obtained by treatment with 0.2% (v/v) Triton X-100 (Sigma) in PBS at 4°C for 20 min, and then incubated with 2 mM *p*-nitrophenyl phosphate (*p*NPP, Sigma) in 1 M diethanolamine at pH 9.8 in the dark at 37°C for 30 min. The absorbance at 405 nm was measured with a plate reader. The total protein content of the lysates was evaluated by BCA assay (Pierce, USA). The ALP activity was calculated by normalization to the protein content of the lysates.

Cytochemical staining

ALP staining. At day 24 of induction with BM or OM, ALP staining was performed. The samples were washed once with PBS and fixed with 5% glutaraldehyde for 15 min. After washing twice with distilled water, a mix solution of BCIP (0.17 mg mL^{-1}, Applichem, Germany) and NBT (0.33 mg mL^{-1}, Applichem) in 0.375 M AMP buffer was added into each well, and left for 1 h in the dark at room temperature. The reaction was stopped by washing with 20 mM EDTA (Biochrom AG), and then thoroughly washed with distilled water to remove the excess dye. Images were taken in transmission mode with an Axiovert 100 equipped with a CCD camera.

Alizarin red and Sudan black staining. Alizarin red staining was performed to observe the calcium phosphate deposition of C3H10T1/2 cells. At day 24 of induction with BM or OM, the samples were washed once with PBS and fixed with 4% paraformaldehyde for 15 min. Thereafter, staining with Alizarin red (2%, pH 4.2, Roth) was performed for 45 min in the dark, and the excess dye was removed by rinsing twice with distilled water. Images were taken in transmission mode with an Axiovert 100 equipped with a CCD camera.

Sudan black staining was further performed to counterstain adipocyte-containing osteogenic cultures whose mineralized matrix has been stained with Alizarin red.[37] Briefly, the Alizarin red staining samples were incubated with 1.2% (w/v) Sudan black solution for 30 min in the dark followed by extensive washing with distilled water. Finally, images were taken in transmission mode with an Axiovert 100 equipped with a CCD camera.

Alcian blue staining. At day 24 of chondrogenic induction, the samples were fixed as described above and incubated with 0.5% (w/v) Alcian blue (Roth) in 3% acetic acid for 1 h in the dark to detect the secretion of GAGs and mucopolysaccharides by C3H10T1/2 cells. The excess dye was removed by washing with distilled water and images were taken with an Axiovert 100 equipped with a CCD camera.

Oil red staining. Oil red staining was performed to investigate the presence of lipid vacuoles in C3H10T1/2 cells. Briefly, at day 14 of induction with 100 ng mL^{-1} BMP-2, the samples were fixed as described above and stained with 0.5% (w/v) Oil red (Roth) for 30 min in the dark. Then, the excess dye was removed by thoroughly washing with distilled water and images were taken in transmission mode with an Axiovert 100 equipped with a CCD camera.

Statistics

All the data are provided as mean values ± standard deviations (SDs) from at least three independent experiments. Statistical analysis was performed using Origin with analysis of variance (ANOVA) test (one way) followed by post hoc Tukey testing. The number of samples has been indicated in the respective figures and tables captions.

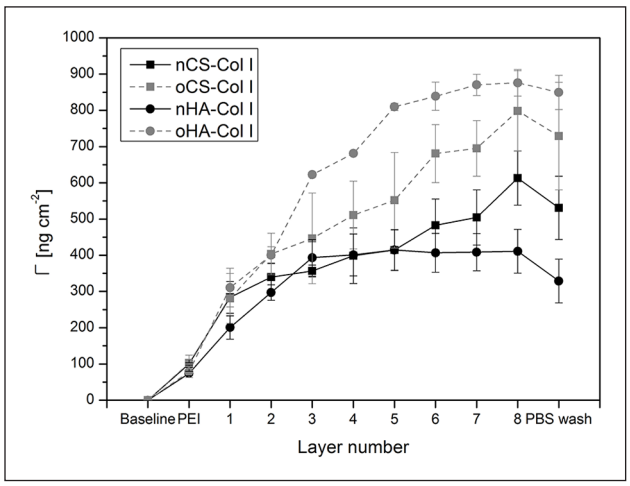

Figure 2. Surface plasmon resonance (SPR) measurements of the layer-by-layer assembly of polyelectrolyte multilayers up to eight layers. Multilayer mass Γ calculated from angle shifts are mean ± SD values of three independent experiments, the initial layer is poly (ethylene imine) (PEI), odd numbers refer to native or oxidized glycosaminoglycans (nGAG or oGAG), even numbers refer to collagen I (Col I).

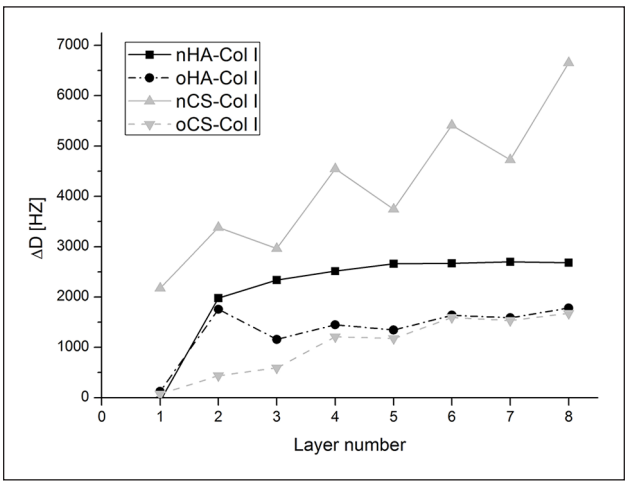

Figure 3. Quartz crystal microbalance (QCM) measurements of damping shift with each polyelectrolyte adsorption steps. The odd numbers refer to native (nGAGs) or oxidized glycosaminoglycans (oGAGs) and even numbers refer to collagen I (Col I). Four bilayers of native hyaluronic acid (nHA), oxidized hyaluronic acid (oHA), native chondroitin sulfate (nCS), or oxidized chondroitin sulfate (oCS) were prepared with collagen I (Col I) as terminal layer.

Statistical significance was considered for $p < 0.05$ and is indicated by asterisks.

Results and discussion

Physicochemical characterization of polyelectrolyte multilayers

The multilayer growth was performed under pH 4 condition as in some of our previous work.[16] Considering the isoelectric point (p*I*) of Col I of around 5.5, it should possess a net positive charge at this pH condition. By contrast, both CS and HA represent polyanions at pH 4, because of the pKa values of about 2–2.5 for CS[38] and 2.9 for HA.[39] Hence, the formation of nGAGs and Col I multilayers at pH 4 should be predominantly dependent on ion pairing. The multilayer growth, based on ion pairing for nGAGs–Col I systems and additional cross-linking via the formation of Schiff's base in oGAGs–Col I systems, was monitored using the surface-sensitive SPR technique. The accumulated layer mass of adsorbed polyelectrolytes with increasing layer number was calculated according to equation (1). The results are depicted in Figure 2. In general, the trend in layer growth was similar for polyelectrolyte multilayers based on the same GAG, either nHA–Col I and oHA–Col I, or nCS–Col I and oCS–Col I. However, slight differences were found in the growth regimes of HA-based multilayers when compared to CS-based multilayers.

For nHA–Col I and oHA–Col I systems, a linear increase in adsorbed mass was found up to three (nHA) or five adsorbed layers (oHA) on top of the PEI priming layer. After that, adsorption reached a plateau indicating that mass adsorption reached an equilibrium. It was visible that multilayer mass of oHA–Col I system was significantly higher due to additional chemical cross-linking.

The multilayer growth of the nCS–Col I and oCS–Col I systems here was roughly linear; this trend was in agreement with a previous report for other polyelectrolytes.[40] Again, a higher mass increase was observed for the multilayer system when fabricated with oCS. Furthermore, here the SPR curves revealed a much larger amount of Col I (even numbers) in comparison to nCS and oCS deposition (odd numbers), which was in contrast to HA-based systems, probably due to the higher charge density of CS compared to HA, which enabled the CS-based systems to bind more Col I. Indeed, the fibrillization of Col I was strongly influenced by the type of GAG as studied by CLSM (see Figure 4). Similar findings were shown in previous work comparing heparin to CS-based multilayers regarding the layer growth and polycation adsorption.[41] Furthermore, the increase in angle shifts was higher for multilayers based on oGAGs compared to their natives, indicating that the intrinsic cross-linking capability makes a major contribution to multilayer formation.[41]

QCM measurements were performed to evaluate mechanical properties of polyelectrolyte multilayers on the sensor surface after each adsorption step. According to the damping shift, assumptions on the mechanical properties of multilayers can be drawn because the higher the damping shift, the softer is the substratum.[34] As shown in Figure 3, the damping shift values for nGAGs and oGAGs multilayer systems varied significantly after each layer adsorption, indicating different mechanical properties of

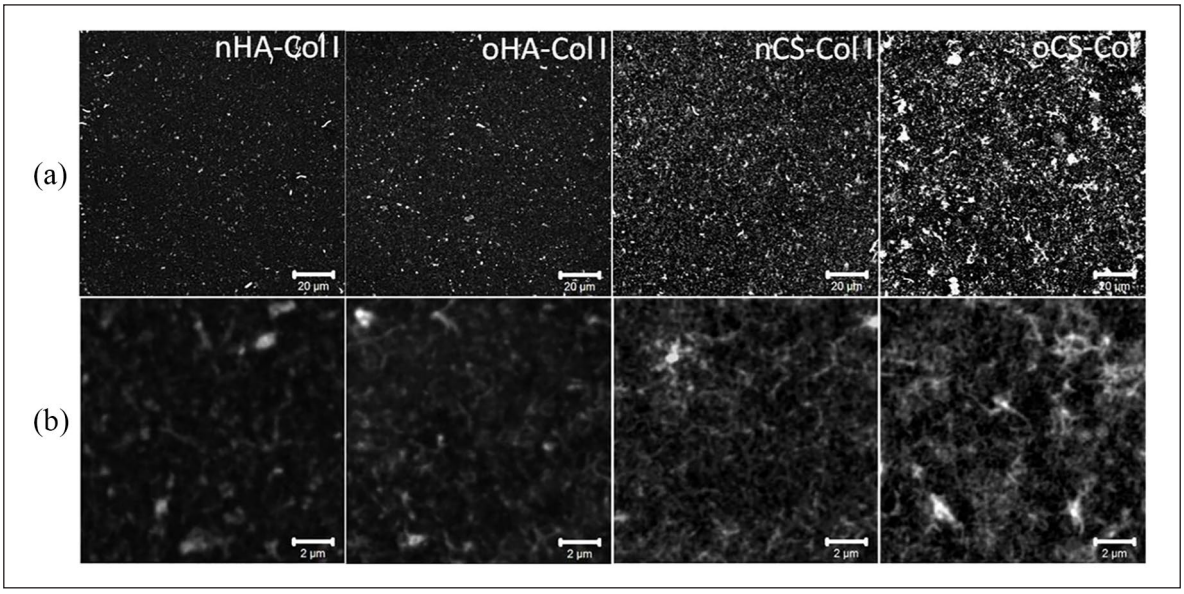

Figure 4. Overall morphology of in situ FITC-labeled collagen I (FITC-Col I) terminated polyelectrolyte multilayers viewed with confocal laser scanning microscopy (CLSM) at (a) lower (scale 20 µm) and (b) higher (scale 2 µm) magnification. Four bilayers of native hyaluronic acid (nHA), oxidized hyaluronic acid (oHA), native chondroitin sulfate (nCS), or oxidized chondroitin sulfate (oCS) were prepared with Col I as polycation.

the polyelectrolyte multilayers. Softer multilayers were obtained when nGAGs were used, as indicated by the pronounced higher damping shifts for both nHA and nCS. Conversely, multilayers made of oGAGs were more rigid because dampening shifts were much lower. Overall, the results demonstrate that the cross-linking significantly affects mechanical features of multilayers, giving rise to stiffer substrata.

To learn more about the ability of GAGs to support fibrillization of Col I in multilayers, the protein was labeled in situ by FITC and multilayers were viewed with CLSM (see Figure 4). Although Col I aggregates were present in all multilayer systems, a prominent fibrous structure was found mostly in CS-based multilayers (both nCS and oCS), showing a tendency to form a network-like structure. Conversely, rather sparse and short fibrils were observed in both nHA and oHA-based multilayers where Col I seemed to form rather discrete aggregates than fibers. Col I fibrillogenesis is known to be affected not only by several environmental parameters such as collagen concentration[42] and pH value,[43] but also by the presence of GAGs such as CS and other naturally derived polyanions.[44] Generally, a pH value above 5.5 normally supports fibrillogenesis of Col I, while at pH value below 5.5 Col I forms more globular structures.[43] Nevertheless, the presence of GAGs, particularly CS, seems to support Col I fibril formation as happened even at pH 4. Furthermore, the concentration of Col I also affects strongly fibril formation as found previously.[42] Presumably CS binds to Col I molecules and promotes the organization of mature fibrils by increasing Col I concentration, as it was observed in the presence of 4,6-disulfated disaccharides structures, previously.[44] In line with this, here, fibril formation in both nCS and oCS-based multilayers was observed, when more Col I was adsorbed.

Adhesion of C3H10T1/2 cells

C3H10T1/2 cells were seeded on the test samples in the absence of serum to allow a direct cell–surface interaction avoiding the interference with other proteins. The quantitative data of cell adhesion and morphology visualized by crystal violet staining and image analysis are shown in Figure 5 and Table 1. It was observed that cells show a superior spreading on the multilayer-coated surfaces, compared to cells on plain glass coverslips, which were used here as additional control to assure normal adhesion of cells. Furthermore, the cells were larger and more elongated on CS-based multilayers in general, and more specifically on oCS-based multilayers when compared to HA-based systems, where cell spreading was significantly lower than on CS-based multilayers. Indeed, significantly more cells adhered on the CS-based multilayer systems (where Col I was dominating) when compared to HA-based systems, while no obvious differences were observed for multilayer systems based on the same GAG type (e.g. nHA and oHA, or nCS and oCS; see Table 1).

Adhesion and spreading of cells are considered as promoters of gene expression and subsequent cell differentiation.[45] To learn more about the organization of C3H10T1/2 cells adhesive machinery, the formation of FA was visualized by staining of vinculin (green, see Figure 6(a)) and the

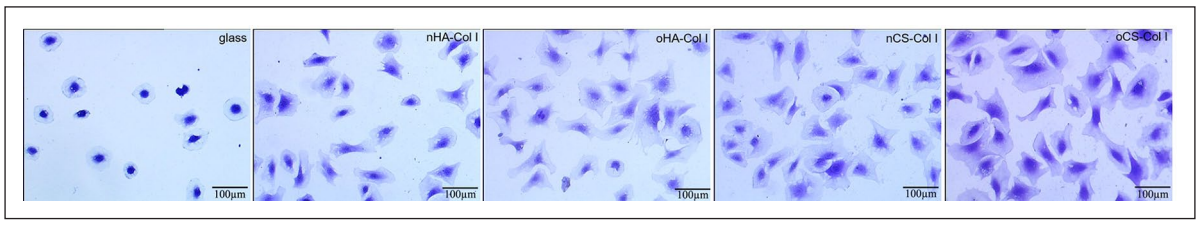

Figure 5. Transmitted light microscopic images of crystal violet staining C3H10T1/2 cells adherent on different test surfaces for 4 h. The cells were seeded in serum-free medium. The four types of polyelectrolyte multilayers are the same as described in Figure 4.

Table 1. Quantification of cell count, area, and aspect ratio of C3H10T1/2 cells seeded on the various multilayers and glass as a control. Results are mean ± SD values of three independent experiments. The four types of polyelectrolyte multilayers are the same as described in Figure 4.

Samples	Cell count (mm^{-2})	Cell area (μm^2)	Aspect ratio (a.u.)
Glass	36.7 ± 9.6	3127.9 ± 1602.4	0.73 ± 0.12
nHA–Col I	41.3 ± 6.3	4875.5 ± 2232.0	0.56 ± 0.14
oHA–Col I	42.6 ± 7.1	5292.0 ± 2952.4	0.53 ± 0.16
nCS–Col I	56.1 ± 6.2	5840.8 ± 2838.1	0.57 ± 0.14
oCS–Col I	54.7 ± 6.2	6025.5 ± 3412.6	0.51 ± 0.15

nHA: native hyaluronic acid; Col I: collagen I; oHA: oxidative hyaluronic acid; nCS: native chondroitin sulfate; oCS: oxidative chondroitin sulfate.

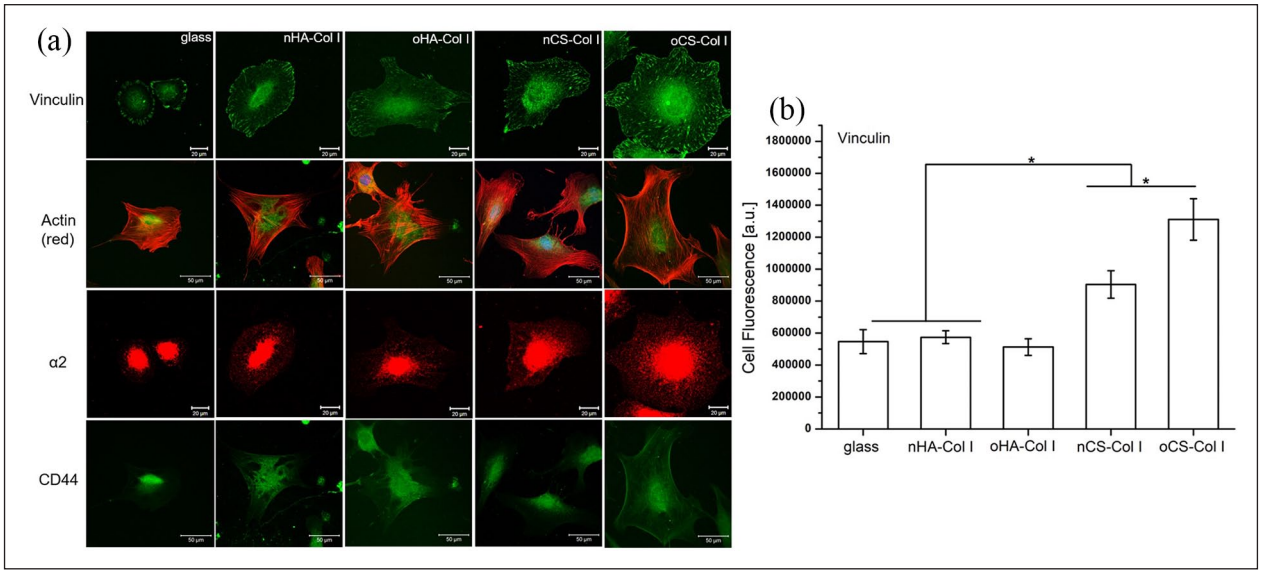

Figure 6. Confocal laser scanning micrographs (CLSM) of C3H10T1/2 cells on different test surfaces. (a) Staining of vinculin, α2, actin (red), and CD44 of C3H10T1/2 cells after 24 h of incubation on different polyelectrolyte multilayers; (b) fluorescence signals of vinculin in focal adhesions quantified by ImageJ and corrected total cell fluorescence was calculated by fluorescence signal with elimination of background signal. The four types of polyelectrolyte multilayers are the same as described in Figure 4.

development of actin cytoskeleton (red, see Figure 6(a)) after 24 h of incubation. Cells cultured on plain glass coverslips displayed short length of vinculin-positive streaks (Figure 6(a)), which were weak in comparison to the cell plated on the multilayers. Though a pronounced cell spreading was observed on all multilayer-coated surfaces, the overall appearance of FA plaques was different. The FA plaques formed on HA-based multilayers were lesser and weaker, which were mainly present at the cell periphery. Conversely, more elongated FA plaques were found on CS-based multilayers and distributed all over the ventral cell side, which is again well in line with the presence of higher quantity and more fibrillar Col I since collagen promotes cell adhesion via integrin-mediated mechanism.[46] Furthermore, the FA plaques were much more pronounced when cells adhered on oCS–Col I (Figure 6(a)). Particularly,

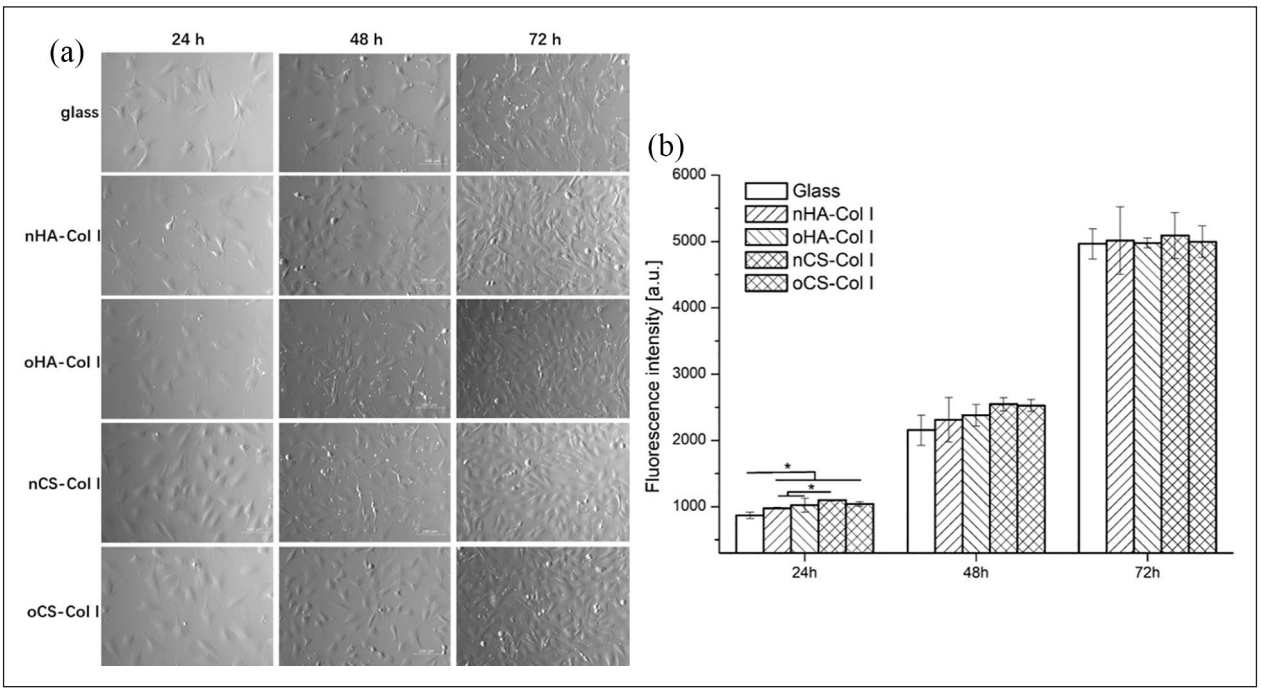

Figure 7. Phase contrast images (a; 100× magnification) and (b) proliferation of long-term C3H10T1/2 cells cultured on plain glass and Col I-terminated multilayers prepared with nHA, oHA, nCS, or oCS as polyanion for 24, 48, and 72 h. Proliferation of C3H10T1/2 cells was assessed by the Qblue assay for determination of metabolically active cells. Results are mean ± SD values of three independent experiments.

the quantitative analysis of vinculin-positive FA showed higher quantities in cells grown on CS–Col I compared to HA–Col I (Figure 6(b)). In addition, more vinculin was pronounced on oCS–Col I compared to the native system nCS–Col I, which is related to the stiffness resulting from intrinsic cross-linking occurring in oGAGs systems, as found by QCM studies (as shown in Figure 6(b)).

Since integrins play a pivotal role in connecting ECM proteins with the cell cytoskeleton and signaling complexes, we further studied the expression and organization of α2 that is regarded as a main collagen receptor[47] and CD44 that is known as a main HA receptor.[48] As shown in Figure 6(a), α2 was more expressed and organized in C3H10T1/2 cells adhering on CS multilayer surfaces (either nCS–Col I or oCS–Col I), while on HA-based surfaces, a weaker expression of α2 with a tendency for perinuclear accumulation was observed (see Figure 6(a) as well). In addition, no large difference was found on the multilayer-coated samples with respect to the expression of CD44, where Col I was used as the terminating layer (Figure 6(a)). However, the expression of α2 and CD44 were always weaker in cells placed on the plain glass coverslips, due to the lack of integrin receptor sites.

Overall, the adhesion, spreading, and α2 integrin organization of C3H10T1/2 cells were increased on CS-based multilayers, which can be explained with the composition of these multilayer systems. First, more Col I was assembled in the CS-based multilayers and formed a well-interconnected fibrillar structure, resembling the natural Col I environment. Col I fibrils have been found to promote the adhesion of a variety of cells via α2 integrin-mediated interaction,[46] which explains also the apparently higher organization of this integrin on CS-based multilayer surfaces. Conversely, apparently lower expression of integrin α2 was found on HA-based multilayers where GAG was dominant as shown also in our previous work leading to the formation of lower quantity of Col I fibrils. In addition, the increased hydrophilicity of HA-based coatings[20] may also lead to the reduced adhesion and spreading of C3H10T1/2 cells, as cells prefer to adhere on surfaces with moderate wettability.[49] It is of note that both spreading and organization of cell adhesion complexes was more pronounced on oCS surfaces when compared to nCS-based multilayers. The additional covalent cross-linking in oGAGs-based systems increased the multilayer stiffness (proven by QCM study), thus, effects on adhesion and spreading of cells can be expected.[50] Nevertheless, the lack of such obvious difference between nHA and oHA multilayers may be due to the higher hydrophilicity of these systems that reduces spreading, and thus overriding the effect of different stiffness of native and oxidized HA-based systems.

Growth of C3H10T1/2 cells on multilayers

To see the effect of multilayers during longer culture of cells, proliferation studies were done with C3H10T1/2 cells for 24, 48, and 72 h. Figure 7(a) shows the morphology and growth of cells during the culture period on plain

glass and Col I-terminated multilayers. As can be seen in Figure 7(a), cells were able to grow on all substrata and cell number increased over time from 24 (left lane) to 72 (right lane) hours, while the cell number was always lower on the plain glass. It was also obvious that cell spreading was improved on CS-based multilayers and combined with a higher cell number as well.

Quantitative data on cell proliferation were obtained with Qblue assay, which determines the metabolic activity of cells. Results in Figure 7(b) show a coincidence with that of adhesion studies and found the quantity of metabolically active cells on plain glass coverslips was lower than that of multilayer-coated surfaces. In addition, improved cell proliferation was detected on CS-based multilayers in comparison to surfaces containing HA, during the first 48 h of incubation. This suggests that surfaces containing higher amounts of Col I fibrils mimic the ECM and thus, support initial cell attachment and growth. However, no obvious differences in amount of metabolically active cells were found between both types of GAG-based multilayers after 48 h incubation. It is assumed that the ability of cells to secrete matrix proteins such as fibronectin may contribute to the lower differences.[51] Furthermore, no significant differences in cell growth were observed between native and oGAGs multilayers, which also indicate that the intrinsic cross-linking ability due to presence of aldehyde groups in oGAGs systems did not have any toxic or other adverse effects on cell proliferation.

Multi-lineages differentiation of C3H10T1/2 cells

Osteogenic differentiation investigation. To see the effect of multilayers on osteogenic differentiation of C3H10T1/2 cells, change of cell morphology was recorded after 24 days of incubation. As can be seen in Figure 8(a), no big difference could be found between the cells cultured in BM, while aggregated vacuoles-like structures resembling probably lipid droplets were observed under OM conditions, especially on the multilayer-coated surfaces.

To evaluate the osteogenic differentiation of C3H10T1/2 cells on the various surfaces, ALP activity was normalized to protein content and investigated at day 10 of post-differentiation (Figure 8(b)). The ALP activity of C3H10T1/2 cells cultured in BM or OM was always lower on the plain glass as compared to the multilayer-coated surfaces. In addition, a higher activity of ALP was found on CS-based multilayers when cells were cultured in BM, though no significant difference was observed. Moreover, it is of note that cells in BM showed significantly higher ALP activity compared to OM, indicating an inhibitory effect of osteogenic supplements on driving osteogenic differentiation of C3H10T1/2 cells (Figure 8(b)). The staining of ALP (Figure 8(c)) was always weaker in cells growing on the plain glass, which is well in line with the quantitative study. Though no intensive staining of ALP could be found on all the samples (either in BM or OM), a slightly stronger staining was observed on CS-based multilayers when cells were cultured in BM that could be related to the higher expression of $\alpha 2$ integrin observed on CS multilayers. The collagen receptors signaling via $\alpha 2\beta 1$ and $\beta 1$ integrins is required for ALP induction process.[52]

Furthermore, at a later stage of osteogenesis, ECM calcification occurs,[52] hence, the deposition of calcium phosphate at day 24 post-differentiation was studied by Alizarin red staining. Figure 8(d) shows that no significant staining was observed when cells cultured in either BM or OM, indicating the limited osteogenic differentiation potential of C3H10T1/2 cells under these conditions. Since pronounced lipid vacuoles were detected in C3H10T1/2 cells when cultured in OM (see in Figure 8(a)), we further studied the adipogenic differentiation of C3H10T1/2 cells by Sudan black staining to counterstain adipocyte-containing osteogenic cultures whose mineralized matrix has been stained with Alizarin red.[37] Indeed, significant staining with Sudan black was observed when C3H10T1/2 cells were cultured in OM (Figure 8(d)), where no positive staining of Alizarin red was found. In addition, the staining with Sudan black was more intensive on oGAGs-based surfaces. This finding provided a hint to a dominating adipogenic compared to osteogenic differentiation of C3H10T1/2 cells, when exposed to medium with osteogenic supplements, such as dexamethasone and BMP-2. By contrast, no significant staining with Sudan black was observed when C3H10T1/2 cells were cultured in BM (Figure 8(d)) indicating that the adipogenesis occurred because of an induction effect caused by the supplements added in case of OM. Previous studies found that BMPs such as BMP-2[29] and BMP-4[53] are capable of triggering commitment of multipotent C3H10T1/2 cells to the adipocyte lineage, which might explain the positive Sudan black staining compared to the negative staining of mineralized matrix that was observed. Furthermore, the synthetic glucocorticoid dexamethasone has a regulatory effect on mesenchymal cells commitment to various cell lineages.[54] The promoting effect of dexamethasone on adipogenesis has been described by others.[55] In cells that are not committed to osteogenic differentiation only, dexamethasone had a stimulatory effect on adipogenesis.[56] Therefore, we concluded that both dexamethasone and BMP-2 supplements in OM might trigger C3H10T1/2 cells more toward adipogenesis.

As the addition of BMP-2 might push C3H10T1/2 cells more toward adipogenesis, we further investigated the effect of BMP-2 alone (no OM or CM supplements) on driving C3H10T1/2 cells differentiation. The cells were cultured in 100 ng mL^{-1} BMP-2 and incubated for 14 days, and then histochemical staining was carried out to view the ECM deposition. As can be seen in Figure 9, no positive staining of Alizarin red or Alcian blue was observed in

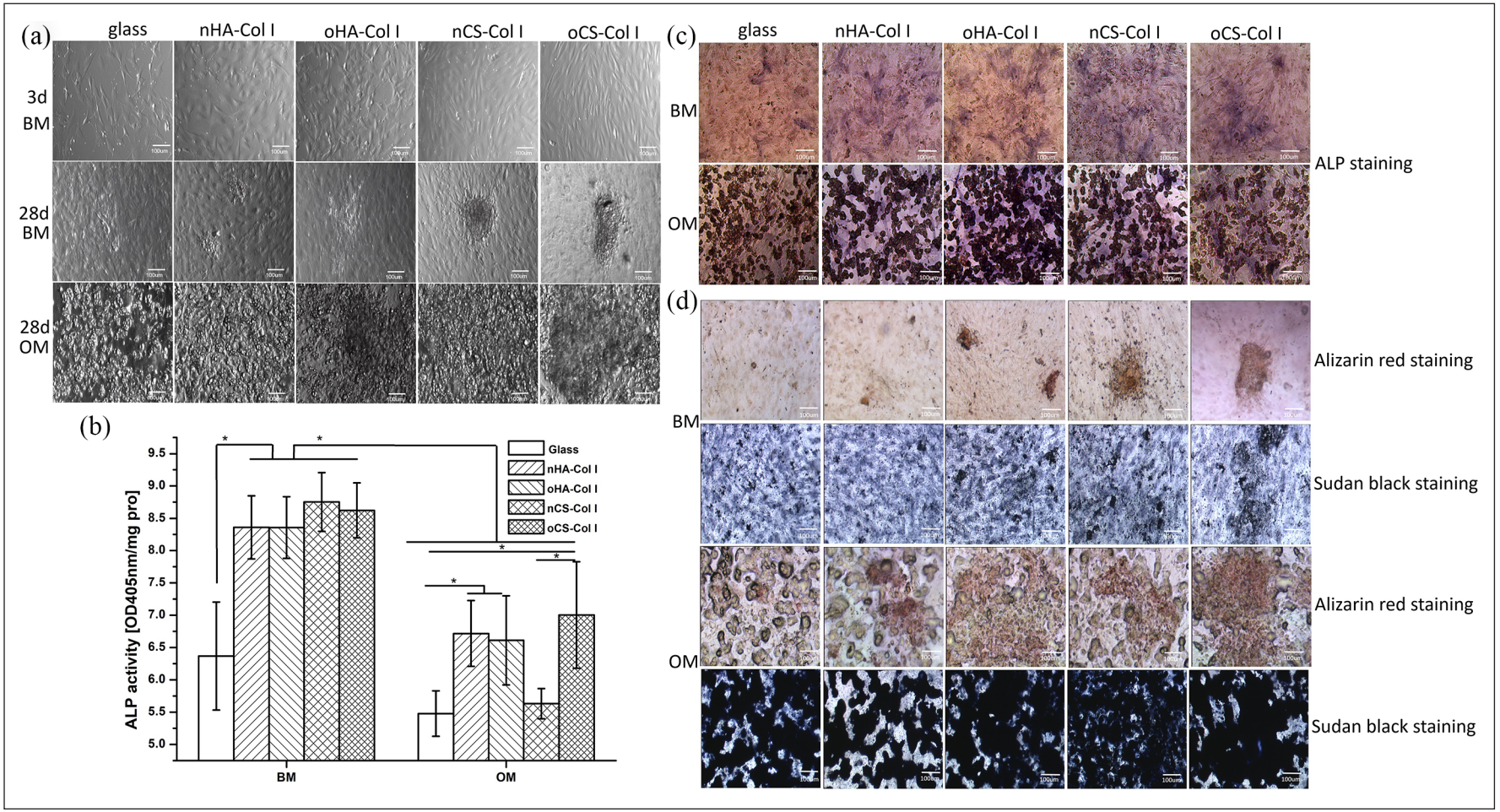

Figure 8. Phase contrast images (a), ALP activity (b), and histochemistry staining ((c) and (d)) of C3H10T1/2 cells cultured on various test samples with basal medium (BM) and osteogenic medium (OM). ALP activity of cells was determined at day 10 post-differentiation; ALP staining and Alizarin red staining were performed at day 24 post-differentiation; Sudan black staining was performed to counterstain adipocyte-containing osteogenic cultures whose mineralized matrix has been stained with Alizarin red. The four types of polyelectrolyte multilayers are the same as described in Figure 4.

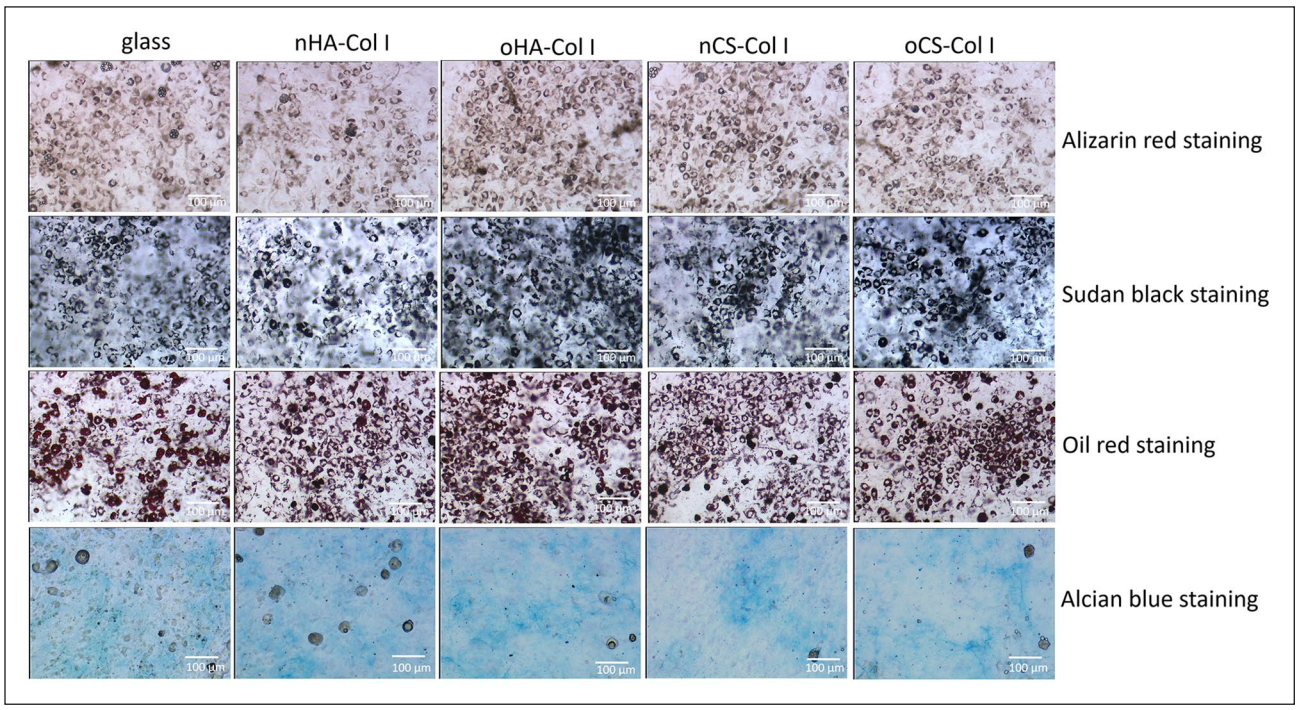

Figure 9. Histochemistry staining of C3H10T1/2 cells placed on various test samples with 100 ng mL^{-1} BMP-2 up to 14 days. The four types of polyelectrolyte multilayers are the same as described in Figure 4.

samples indicating no osteogenic or chondrogenic differentiation of C3H10T1/2 cells. By contrast, with respect to adipogenic markers, Oil red and Sudan black staining revealed lipid vacuoles in cells, especially when they were cultured on the multilayer-coated surfaces. This shows the effect of BMP-2 in directing C3H10T1/2 cells commitment to adipogenesis, as it has also been observed by others, too.[57] BMP-2 initiates this adipogenic commitment via activating of downstream signaling intermediates of BMP signaling pathway through increasing their expression and phosphorylation.[57] Moreover, the development of fat droplets was more pronounced on the oGAGs multilayers.

Chondrogenic differentiation investigation. To see the effect of multilayers on chondrogenic differentiation of C3H10T1/2 cells, cell morphology was recorded after 24 days of incubation. No large differences could be found between cells cultured in BM as shown in Figure 10(a). However, in note contrast, only few cells adhered and mostly presented a round-shaped morphology under CM condition as it has been observed for MSCs in other studies.[58]

To further view the deposition of a cartilage-specific matrix, C3H10T1/2 cells were stained with Alcian blue at day 24 post-differentiation (Figure 10(b)). A positive staining with Alcian blue was observed on multilayer-coated surfaces when cells were cultured in BM. This staining was more intensive on HA-based multilayers, especially on nHA surfaces. In note contrast, no significant staining could be detected when cells were grown in CM, most of the cells seemed to detach or shrink on the multilayer-coated surfaces, suggesting that chondrogenic supplements, probably dexamethasone, impeded chondrogenic differentiation of C3H10T1/2 cells. Treatment of tendon stem cells with dexamethasone has been found to increase the expression of PPARγ gene, which is a specific marker for adipogenesis of adult stem cells.[59] Other studies also showed that dexamethasone suppressed chondrocytes differentiation when it was in combination with ITS by modulating the local environment,[60] which could be the case here since our chondrogenic medium was supplemented with ITS together with dexamethasone.

Overall, the osteogenic differentiation of C3H10T1/2 cells was increased on CS-based multilayers, while the chondrogenic differentiation was more pronounced on HA-based systems, but only when cells were cultured in BM. Conversely, C3H10T1/2 cells displayed a limited differentiation potential toward osteogenic and chondrogenic lineages when cultured in media with osteogenic or chondrogenic supplements. C3H10T1/2 cells differentiated more into an adipogenic lineage, when cultured in OM or with addition of 100 ng mL^{-1} BMP-2 to BM, and it was more pronounced on oGAGs multilayers. We assumed that the differed differentiation potential of C3H10T1/2 cells in BM, toward osteogenic and chondrogenic lineages on multilayer-coated surfaces, was mostly dependent on the molecular composition of the multilayers where the observed effect on cells was only because of the intrinsic

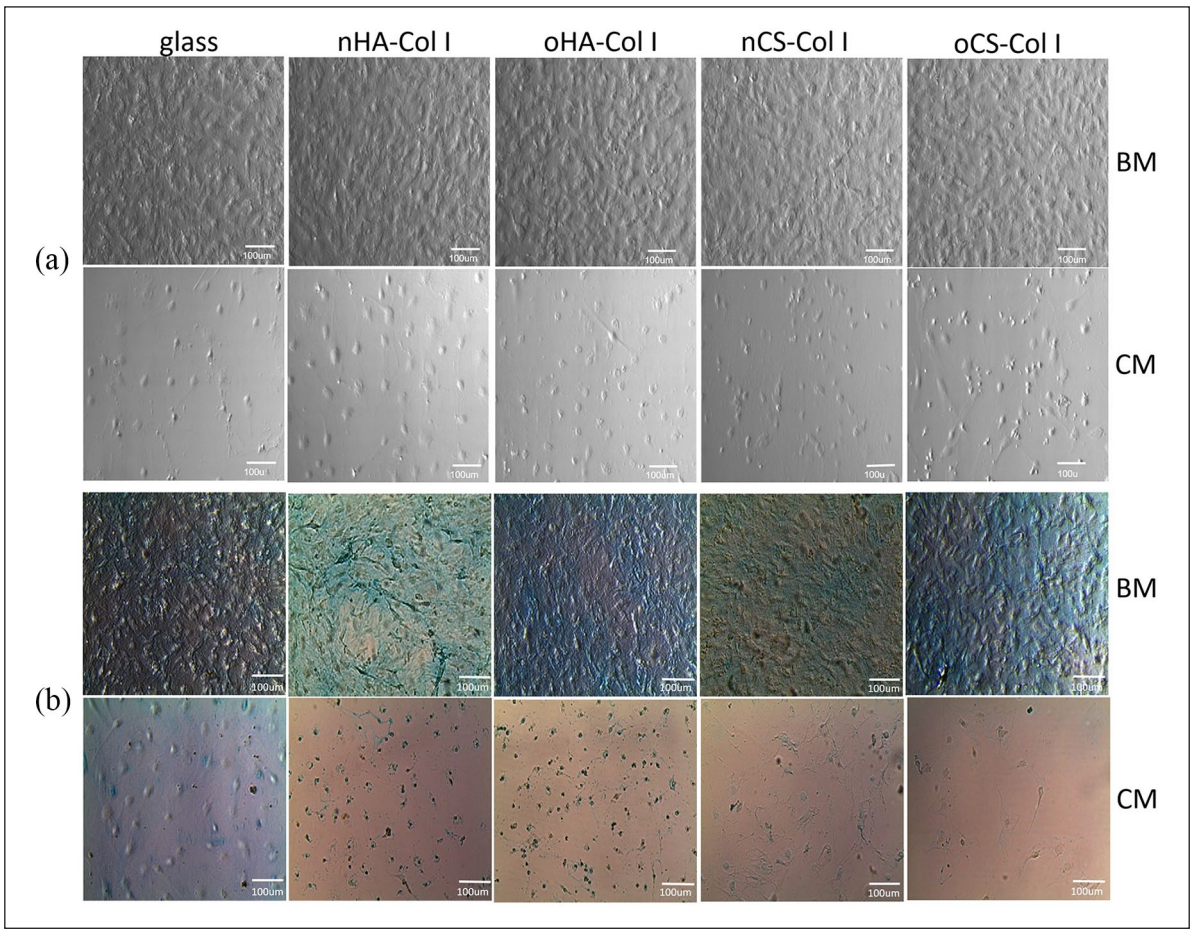

Figure 10. Phase contrast images (a) and Alcian blue staining (b) of C3H10T1/2 cells placed on various test samples supplied with basal medium (BM) and chondrogenic medium (CM), respectively. Staining was performed at day 24 post-differentiation. The four types of polyelectrolyte multilayers are the same as described in Figure 4.

properties of the multilayer surfaces without any external addition. The larger quantity and fibrillar structure of Col I, which is also a key component of bone, contributed to more osteogenic differentiation of C3H10T1/3 cells on CS-based multilayers. This was also evidenced by enhanced cell-material interactions, such as FA formation and α2 integrin clustering, while interaction of cells with Col I via α2 integrin has been shown to be important in regulating osteogenic differentiation.[61] However, many studies demonstrated the benefits of HA and CS on cartilage formation and bone regeneration, respectively.[62] It was found that the type of GAG can be used for controlling the lineage specification of MSCs, whereby CS enhanced the osteogenic differentiation of MSCs, and HA promoted chondrogenic differentiation.[62] In addition, the differentiation of C3H10T1/2 cells toward adipocytes might be attributed to the presence of BMP-2,[29] and dexamethasone,[56] which have been found to promote adipogenesis. Furthermore, the ALP activity of cells in OM (Figure 8(b)) despite their adipogenic differentiation behavior observed by histochemical staining (Figure 8(d)), does not contradict the overall findings. ALP has been shown to be upregulated during osteogenic and adipogenic differentiation. It cannot be considered as lineage specific marker as it only proves the starting of differentiation.[63] Presumably, the most pronounced adipogenesis observed on oGAGs multilayers might be related to a different interaction of BMP-2 with oxidized multilayers, where the activity of the growth factor is extremely enhanced as shown in a previous study from our group.[41]

Conclusion

It was shown that the adhesion and differentiation of C3H10T1/2 cells were largely affected by the composition of polyelectrolyte multilayers. The CS-based multilayers rich in larger quantity and fibrillar structure of Col I have a superior effect on promoting cell adhesion in terms of increased FA formation and α2 integrin clustering, and osteogenic differentiation, when cultured in BM without any osteogenic supplements. It was also found that multilayers made of oGAGs and Col I possessed a higher rigidity resulting from intrinsic cross-linking, which affected spreading of cells. By contrast, the chondrogenic

differentiation of C3H10T1/2 cells was more pronounced on HA-based polyelectrolyte multilayers. Furthermore, it is of note that the CM and OM supplemented with BMP-2 and dexamethasone, impeded the chondrogenic and osteogenic differentiation of C3H10T1/2 cells. Conversely, the BMP-2 and dexamethasone supplemented OM and BMP-2 alone directed adipogenic differentiation of C3H10T1/2 cells, which was more evident on oGAGs multilayers. These findings provided new insights to our understanding not only the importance of controlling matrix composition as an approach to manipulate cell fates but also the selection of C3H10T1/2 cells for differentiation investigations. Cautions are needed when using C3H10T1/2 cells for osteogenic and chondrogenic studies.

Declaration of conflicting interests

The author(s) declared no potential conflicts of interest with respect to the research, authorship, and/or publication of this article.

Funding

The author(s) disclosed receipt of the following financial support for the research, authorship, and/or publication of this article: This work was funded partly by the National Natural Science Foundation of China (31600772); Natural Science Foundation of Guangdong Province, China (2019A1515011613, 2017A03 0313176); and the Zhanjiang competitive funding project, China (2018A01032). This work was also partly supported by the Characteristic innovation projects of Guangdong Province universities (2018KTSCX076), the Stem Cell Preclinical Research Project of Affiliated Hospital of Guangdong Medical University, China (2018PSSC002), and the Summit project of high-level hospital construction of Affiliated Hospital of Guangdong Medical University (2019083044). This work was done in the frame of the International Graduate School AGRIPOLY supported by the European Regional Development Fund (ERDF) and the Federal State Saxony-Anhalt.

ORCID iD

Mingyan Zhao https://orcid.org/0000-0003-4063-8351

References

1. Frantz C, Stewart KM and Weaver VM. The extracellular matrix at a glance. *Journal of Cell Science* 2010; 123: 4195.
2. Schnabelrauch M, Scharnweber D and Schiller J. Sulfated glycosaminoglycans as promising artificial extracellular matrix components to improve the regeneration of tissues. *Curr Med Chem* 2013; 20(20): 2501–2523.
3. Schaefer LSR. Proteoglycans: from structural compounds to signaling molecules. *Cell Tissue Res* 2010; 339(1): 237–246.
4. Kechagia JZ, Ivaska J and Roca-Cusachs P. Integrins as biomechanical sensors of the microenvironment. *Nat Rev Mol Cell Biol* 2019; 20(8): 457–473.
5. Sainio A and Järveläinen H. Extracellular matrix-cell interactions: focus on therapeutic applications. *Cell Signal* 2020; 66: 109487.
6. Hynes RO. The extracellular matrix: not just pretty fibrils. *Science* 2009; 326: 1216.
7. Liu ZM, Gu Q, Xu ZK, et al. Synergistic effect of polyelectrolyte multilayers and osteogenic growth medium on differentiation of human mesenchymal stem cells. *Macromol Biosci* 2010; 10: 1043–1054.
8. Liu Z-M, Lee S-Y, Sarun S, et al. Biocompatibility of poly (L-lactide) films modified with poly (ethylene imine) and polyelectrolyte multilayers. *J Biomater Sci Polym* 2010; 21(6–7): 893–912.
9. Ma Z, Mao Z and Gao C. Surface modification and property analysis of biomedical polymers used for tissue engineering. *Colloid Surf B: Biointerf* 2007; 60: 137–157.
10. Hao L and Lawrence J. *Laser surface treatment of bio-implant materials*. Chichester: Wiley, 2005.
11. Roach P, Eglin D, Rohde K, et al. Modern biomaterials: a review—bulk properties and implications of surface modifications. *J Mater Sci Mater Med* 2007; 18(7): 1263–1277.
12. Rahmany MB and Van Dyke M. Biomimetic approaches to modulate cellular adhesion in biomaterials: A review. *Acta Biomater* 2013; 9(3): 5431–5437.
13. Niepel MS, Almouhanna F, Ekambaram BK, et al. Cross-linking multilayers of poly-l-lysine and hyaluronic acid: Effect on mesenchymal stem cell behavior. *Int J Artif Organs* 2018; 41(4): 223–235.
14. Ren KF, Hu M, Zhang H, et al. Layer-by-layer assembly as a robust method to construct extracellular matrix mimic surfaces to modulate cell behavior. *Progress in Polymer Science* 2019; 92: 1–34.
15. Silva JM, Reis RL and Mano JF. Biomimetic extracellular environment based on natural origin polyelectrolyte multilayers. *Small* 2016; 12(32): 4308–4342.
16. Guillot R, Gilde F, Becquart P, et al. The stability of BMP loaded polyelectrolyte multilayer coatings on titanium. *Biomaterials* 2013; 34(23): 5737–5746.
17. Zhao M, Altankov G, Grabiec U, et al. Molecular composition of GAG-collagen I multilayers affects remodeling of terminal layers and osteogenic differentiation of adipose-derived stem cells. *Acta Biomaterialia* 2016; 41: 86–99.
18. Aggarwal N, Altgärde N, Svedhem S, et al. Tuning cell adhesion and growth on biomimetic polyelectrolyte multilayers by variation of pH during layer-by-layer assembly. *Macromol Biosci* 2013; 13(10): 1327–1338.
19. Chaubaroux C, Vrana E, Debry C, et al. Collagen-based fibrillar multilayer films cross-linked by a natural agent. *Biomacromolecules* 2012; 13: 2128–2135.
20. Zhao M, Li L, Zhou C, et al. Improved stability and cell response by intrinsic cross-linking of multilayers from collagen I and oxidized glycosaminoglycans. *Biomacromolecules* 2014; 15: 4272–4280.
21. Tuan RS, Boland G and Tuli R. Adult mesenchymal stem cells and cell-based tissue engineering. *Arthritis Res Ther* 2002; 5: 32.
22. Uygun BE, Stojsih SE and Matthew HW. Effects of immobilized glycosaminoglycans on the proliferation and differentiation of mesenchymal stem cells. *Tissue Eng Part A* 2009; 15(11): 3499–3512.
23. Danišovič I, Varga Ľ and Polák Š. Growth factors and chondrogenic differentiation of mesenchymal stem cells. *Tissue and Cell* 2012; 44: 69–73.
24. Trivanović D, Jauković A, Popović B, et al. Mesenchymal stem cells of different origin: comparative evaluation of

proliferative capacity, telomere length and pluripotency marker expression. *Life Sci* 2015; 141: 61–73.
25. Reznikoff CA, Brankow DW and Heidelberger C. Establishment and characterization of a cloned line of C3H mouse embryo cells sensitive to postconfluence inhibition of division. *Cancer Res* 1973; 33(12): 3231–3238.
26. Katagiri T, Ikeda T, Yoshiki S, et al. The non-osteogenic mouse pluripotent cell line, C3H10T1/2, is induced to differentiate into osteoblastic cells by recombinant human bone morphogenetic protein-2. *Biochem Biophys Res Commun* 1990; 172: 295–299.
27. Atkinson BL, Benedict JJ, Huffer WE, et al. Combination of osteoinductive bone proteins differentiates mesenchymal C3H/10T1/2 cells specifically to the cartilage lineage. *J Cell Biochem* 1997; 65: 325–339.
28. Tang QQ, Otto TC and Lane MD. Commitment of C3H10T1/2 pluripotent stem cells to the adipocyte lineage. *Proc Natl Acad Sci USA* 2004; 101: 9607–9611.
29. Chun XCQ, Yang S, Sun F, et al. BMP2 Induces Adipogenic Differentiation of C3 H10T1/2 Cells. *Chin J Biochem Mol Biol* 2008; 24: 142–147.
30. Baudequin T, Gaut L, Mueller M, et al. The osteogenic and tenogenic differentiation potential of C3H10T1/2 (Mesenchymal Stem Cell Model) cultured on PCL/PLA electrospun scaffolds in the absence of specific differentiation medium. *Materials* 2017; 10: 1387.
31. Fung CD, Cheung PW, Ko WH, et al. *Micromachining and micropackaging of transducers*. Amsterdam: Elsevier, 1985.
32. Niepel MS, Peschel D, Sisquella X, et al. pH-dependent modulation of fibroblast adhesion on multilayers composed of poly(ethylene imine) and heparin. *Biomaterials* 2009; 30(28): 4939–4947.
33. Schasfoort RBM and Tudos Anna J. *Handbook of Surface Plasmon Resonance*. Cambridge: Royal Society of Chemistry, 2008, pp. 35–80.
34. Kirchhof K, Andar A, Yin HB, et al. Polyelectrolyte multilayers generated in a microfluidic device with pH gradients direct adhesion and movement of cells. *Lab Chip* 2011; 11: 3326–3335.
35. Höök F. *Development of a Novel QCM Technique for Protein Adsorption Studies*. PhD thesis, Chalmers University of Technology and Göteborg University, Gothenburg, 1997.
36. McSwain BS, Irvine RL, Hausner M, et al. Composition and distribution of extracellular polymeric substances in aerobic flocs and granular sludge. *Appl Environ Microbiol* 2005; 71(2): 1051–1057.
37. Vemuri MC, Chase LG and Rao MS. Mesenchymal stem cell assays and applications. In: Walker JM (ed.) *Methods in molecular biology*. Totowa, NJ: Humana Press, 2011.
38. Kuettner KE and Lindenbaum A. Analysis of mucopolysaccharides in partially aqueous media. *Biochim Biophys Acta* 1965; 101: 223–225.
39. Almodóvar J, Place LW, Gogolski J, et al. Layer-by-layer assembly of polysaccharide-based polyelectrolyte multilayers: a spectroscopic study of hydrophilicity, composition, and ion pairing. *Biomacromolecules* 2011; 12: 2755–2765.
40. Mhanna RF, Vörös J and Zenobi-Wong M. Layer-by-Layer Films Made from Extracellular Matrix Macromolecules on Silicone Substrates. *Biomacromolecules* 2011; 12: 609–616.
41. Anouz R, Repanas A, Schwarz E, et al. Novel surface coatings using oxidized glycosaminoglycans as delivery systems of bone morphogenetic protein 2 (BMP-2) for bone regeneration. *Macromol Biosci* 2018; 18(11): e1800283.
42. Raspanti M, Viola M, Sonaggere M, et al. Collagen fibril structure is affected by collagen concentration and decorin. *Biomacromolecules* 2007; 8(7): 2087–2091.
43. Jiang F, Hörber H, Howard J, et al. Assembly of collagen into microribbons: effects of pH and electrolytes. *J Struct Biol* 2004; 148(3): 268–278.
44. Kvist AJ, Johnson AE, Mörgelin M, et al. Chondroitin sulfate perlecan enhances collagen fibril formation. Implications for perlecan chondrodysplasias. *J Biol Chem* 2006; 281: 33127–33139.
45. McBeath R, Pirone DM, Nelson CM, et al. Cell shape, cytoskeletal tension, and RhoA regulate stem cell lineage commitment. *Dev Cell* 2004; 6(4): 483–495.
46. Coelho NM, González-García C, Planell JA, et al. Different assembly of type IV collagen on hydrophilic and hydrophobic substrata alters endothelial cells interaction. *Eur Cell Mater* 2010; 19: 262–272.
47. Gullberg DE and Lundgren-Åkerlund E. Collagen-binding I domain integrins—what do they do? *Prog Histochem Cytochem* 2002; 37: 3–54.
48. Ouasti S, Kingham PJ, Terenghi G, et al. The CD44/integrins interplay and the significance of receptor binding and re-presentation in the uptake of RGD-functionalized hyaluronic acid. *Biomaterials* 2012; 33(4): 1120–1134.
49. Köwitsch A, Yang Y, Ma N, et al. Bioactivity of immobilized hyaluronic acid derivatives regarding protein adsorption and cell adhesion. *Biotechnol Appl Biochem* 2011; 58(5): 376–389.
50. Richert L, Engler AJ, Discher DE, et al. Elasticity of native and crosslinked polyelectrolyte multilayer films. *Biomacromolecules* 2004; 5: 1908–1916.
51. Altankov GGT. Fibronectin matrix formation by human fibroblasts on surfaces varying in wettability. *J Biomater Sci Polym* 1996; 8(4): 299–310.
52. Jikko A, Harris SE, Chen D, et al. Collagen integrin receptors regulate early osteoblast differentiation induced by BMP-2. *J Bone Miner Res* 1999; 14(7): 1075–1083.
53. Zhao GL, Li G, Chan KM, et al. Comparison of multipotent differentiation potentials of murine primary bone marrow stromal cells and mesenchymal stem cell line C3H10T1/2. *Calcif Tissue Int* 2009; 84(1): 56–64.
54. Ghali O, Broux O, Falgayrac G, et al. Dexamethasone in osteogenic medium strongly induces adipocyte differentiation of mouse bone marrow stromal cells and increases osteoblast differentiation. *BMC Cell Biology* 2015; 16: 9.
55. Lee SY, Lim J, Khang G, et al. Enhanced Ex vivo expansion of human adipose tissue–derived mesenchymal stromal cells by fibroblast growth factor-2 and dexamethasone. *Tissue Eng Part A* 2009; 15(9): 2491–2499.
56. Ito S, Suzuki N, Kato S, et al. Glucocorticoids induce the differentiation of a mesenchymal progenitor cell line, ROB-C26 into adipocytes and osteoblasts, but fail to induce terminal osteoblast differentiation. *Bone* 2007; 40(1): 84–92.
57. Huang H, Song TJ, Li X, et al. BMP signaling pathway is required for commitment of C3H10T1/2 pluripotent stem cells to the adipocyte lineage. *Proc Natl Acad Sci* 2009; 106: 12670–12675.

58. Chen G, Akahane D, Kawazoe N, et al. Chondrogenic differentiation of mesenchymal stem cells in a leakproof collagen sponge. *Mater Sci Eng: C* 2008; 28: 195–201.
59. Zhang J, Keenan C and Wang JH. The effects of dexamethasone on human patellar tendon stem cells: Implications for dexamethasone treatment of tendon injury. *J Orthop Res* 2013; 31(1): 105–110.
60. Naito M, Ohashi A and Takahashi T. Dexamethasone inhibits chondrocyte differentiation by suppression of Wnt/β-catenin signaling in the chondrogenic cell line ATDC5. *Histochem Cell Biol* 2015; 144(3): 261–272.
61. Salasznyk RM, Klees RF, Hughlock MK, et al. ERK signaling pathways regulate the osteogenic differentiation of human mesenchymal stem cells on collagen I and vitronectin. *Cell Commun Adhes* 2004; 11(5–6): 137–153.
62. Murphy CM, Matsiko A, Haugh MG, et al. Mesenchymal stem cell fate is regulated by the composition and mechanical properties of collagen–glycosaminoglycan scaffolds. *J Mech Behav Biomed Mater* 2012; 11: 53–62.
63. Köllmer M, Buhrman JS, Zhang Y, et al. Markers are shared between adipogenic and osteogenic differentiated mesenchymal stem cells. *J Develop Biol Tissue Eng* 2013; 5: 18.